

# Scanning Tunneling Microscopy in TTF-TCNQ :direct proof of phase and amplitude modulated charge density waves

Z. Z. Wang,<sup>1</sup> J. C. Girard,<sup>1</sup> C. Pasquier,<sup>2</sup> D. Jérôme,<sup>2</sup> and K. Bechgaard<sup>3</sup>

<sup>1</sup>*Laboratoire de Photonique et de Nanostructures,  
CNRS, route de Nozay, 91460, Marcoussis, France*

<sup>2</sup>*Laboratoire de Physique des Solides (CNRS),  
Université Paris-Sud, 91405, Orsay, France*

<sup>3</sup>*Polymer Science Department, Research Center Risø, DK 4000, Roskilde, Denmark*

(Dated: March 20, 2018)

## Abstract

Charge density waves (CDW) have been studied at the surface of a cleaved TTF-TCNQ single crystal using a low temperature scanning tunneling microscope (STM) under ultra high vacuum (UHV) conditions, between 300K and 33K with molecular resolution. All CDW phase transitions of TTF-TCNQ have been identified. The measurement of the modulation wave vector along the  $\mathbf{a}$  direction provides the first evidence for the existence of domains comprising single plane wave modulated structures in the temperature regime where the transverse wave vector of the CDW is temperature dependent, as hinted by the theory more than 20 years ago.

The discovery of the organic molecular crystal tetrathiafulvalene-tetracyanoquinodimethane (TTF-TCNQ), comprising weakly coupled one dimensional (1D) molecular stacks, created a tremendous turmoil in 1973 [1, 2]. This was the first molecular crystal to show a conductivity approaching that of conventional metals at room temperature and exhibiting a metal-like behaviour on cooling. A partial charge is transferred from TTF to TCNQ stacks and the charge density  $\rho$  potentially available for transport is determined by the value of  $k_F$  at which the bonding TCNQ band crosses the antibonding TTF band, leading to  $2k_F = \rho\pi/b$  in the 1D band picture, where  $b$  is the unit cell length. Between 54K and 38K, CDW's successively develop in the TCNQ and TTF stacks. These transitions have been ascribed to the instability of a one dimensional electronic gas due to the Peierls mechanism, *see reference* [3] for a review.

When the CDW's are active on both kinds of stacks frustration arises and the 2D ordered superlattice can be described by plane waves with the wave vectors  $q_+ = [+q_a(T), 2k_F]$  or  $q_- = [-q_a(T), 2k_F]$ . Both lead to configurations which are energetically equivalent. The wave vector  $q_+$  gives rise to a charge modulation such as  $\rho(r) = \rho_+ \cos(q_+ r + \theta_+)$  which is a CDW of fixed amplitude and a phase varying like  $q_a a$  along the  $a$  direction, and similarly for the  $q_-$  wave vector. Consequently, the diffraction pattern of the CDW state should display an equal number of domains characterized by the vectors  $q_+$  and  $q_-$ .

There also exists another possibility, namely: the superposition of the two plane waves  $q_+$  and  $q_-$  which leads to a CDW with constant phase but a modulated amplitude along the  $a$  direction [4, 5], double- $q$  configuration. The only solution which can take advantage of the commensurability energy related to the transverse commensurate periodicity through the fourth order Umklapp term in a Landau-Ginzburg expansion is the double- $q$  configuration [5]. This means that both wave vectors are simultaneously activated below 38 K with four satellite spots at  $\pm q_+$  and  $\pm q_-$  in the reciprocal space around a main Bragg spot. On the other hand, it has been pointed out that the phase modulated solution should be the most stable one in the incommensurate transverse wave vector temperature regime and also the only one to provide a smooth onset at 49K [5]. The presence of a microscopic coexistence of vectors  $q_+$  and  $q_-$  below 38K has been shown by X-ray diffuse scattering [6] and a structural determination [7]. However, in spite of the data of an early STM study of TTF-TCNQ [8] showing a phase modulated 2D structure at 42 K there exists no direct evidence of a transition from a phase modulated regime between 49 and 38 K where the temperature

dependence makes the amplitude of  $q_a$  sliding to an amplitude modulated situation below 38 K. Diffraction experiments performed on a bulk sample have failed to provide a clue since they cannot tell the difference between an amplitude modulated configuration and one in which the phase is modulated with an equal number of domains with  $q_+$  and  $q_-$ . Therefore, only those specific techniques like STM probing the sample locally are likely to provide an answer to this problem.

The present STM investigation of a TTF-TCNQ single crystal has been performed in a broad temperature range (33-300 K). The primary goal was to achieve the best possible experimental conditions in order to provide local information regarding the development of 3D ordered CDW's below 54K. This work brings the first direct experimental proof for the existence of phase modulated and amplitude modulated CDW's between 49-38 K and below 38 K respectively and also supports the model proposed by theoreticians more than 20 years ago [4, 9].

The experiment was carried out in an UHV-LT-STM system with separate UHV chambers for STM measurements, sample and tip preparation. The base pressure in each chamber is in the range of  $10^{-11}$  mbar. A commercially available LT-STM head is used in this study and the entire scanning unit (including tip, sample, piezo tube, piezo motor and damping system) is inserted in a thermostat with four gold-plated cold shields (Omicron LT-STM). The sample temperature is controlled by a Lake Shore DRC 91C controller. Typical temperature fluctuations are less than 20 mK in 200 seconds with an average temperature drift below 50 mK per hour. Mechanically sharpened Pt/Ir tips were used. The durability of the tips has been demonstrated by their ability to get molecular resolution of TTF-TCNQ for hours. The quality of the tips is checked by their ability to obtain atomic resolution on a gold surface before and after imaging of TTF-TCNQ . We image the sample using a constant current mode. The maximum data rate is 100 KHz and the typical time needed to record one image is 200 seconds.

Crystals of TTF-TCNQ with nice looking natural faces and typical dimensions of  $3 \times 0.5 \times 0.05$  mm<sup>3</sup> are selected for this experiment. A clean (001) surface is obtained by cleaving the single crystal with a razor blade in air just before insertion. Direct exposure to air is restricted to less than 2 minutes. In order to avoid micro-cracks in TTF-TCNQ while cooling or warming, the temperature variation rate is kept at 1 K per minute.

Figure 1a displays a typical image of the **a-b** plane (area  $5.3 \times 5.3$  nm<sup>2</sup>) obtained in

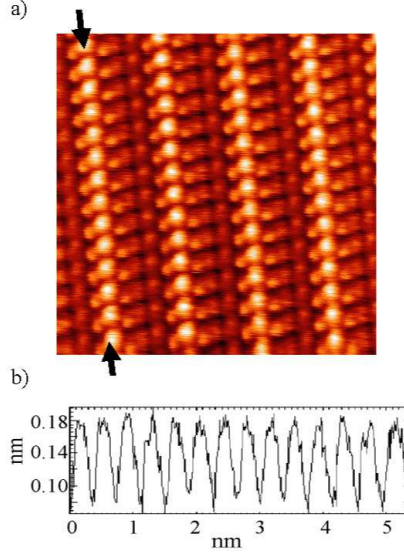


FIG. 1: a) STM image of the **a-b** plane of TTF-TCNQ taken at 63K. The image area is  $5.3 \text{ nm} \times 5.3 \text{ nm}$ . b) shows the profile along a TCNQ stack indicated by black arrows.

a constant current mode ( $I=1 \text{ nA}$ ,  $V=50 \text{ mV}$ ) at  $63 \text{ K}$  where a 1D structure of parallel chains is clearly observed with one set of chains containing a triplet of balls and the other a doublet. According to the calibration of the piezo at low temperature, the distance between similar chains is  $1.22 \text{ nm}$  and  $0.38 \text{ nm}$  between units along the chain direction, see fig.1b. Both distances compare very well with the **a** and **b** lattice constants,  $b = 0.3819 \text{ nm}$  and  $a = 1.229 \text{ nm}$  [10]. We can ascribe the triplet feature in fig.1a to the TCNQ in agreement with the early work of Sleator and Tycko [11]. The TTF molecule appears usually as a single ball feature in STM imaging although reports of doublet structures have also been made in the literature [12]. An extensive interpretation of the TTF-TCNQ image in the absence of CDW will be given in a forthcoming paper[13]and the present work is restricted to the physics provided by STM images of the TCNQ molecules only. No bias voltage dependence (polarity) of the image was observed during our measurements in agreement with the expected conducting nature of the surface [14]. In the whole temperature domain where the sample is metallic *i.e.* above  $54\text{K}$ , images like fig.1a were observed and we could not detect any modulation on the STM image besides that provided by the uniform TTF-TCNQ lattice. Therefore, the periodic modulation along the TCNQ stacks reported in ref [8] at  $61\text{K}$  could be related to static CDW's stabilized by defects or steps on the surface as noticed by the authors.

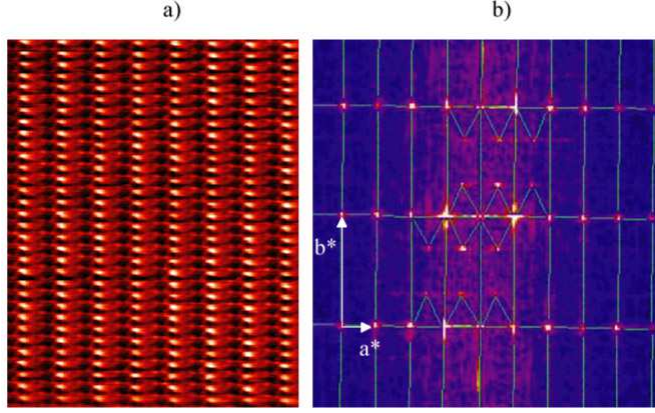


FIG. 2: a) STM image of the **a-b** plane of TTF-TCNQ taken at 49.2K. The image area is 8.7 nm x 11.9 nm, b) Fourier transformed pattern showing the  $2a \times 3.39b$  CDW ordering.

Below 54K a two dimensional superstructure restricted to the TCNQ chains with a period of  $2a \times 3.3b$  appears in the image (see fig.2a).

The modulation wavevector (shown in fig.2b by Fourier transforming the image) does not vary down to 49K. On further cooling, the transverse modulation vector becomes incommensurate (IC) and a temperature dependence  $q_a(T)$  is observed without noticeable change along **b**, figs.3a,b. The Fourier transformed image shows that the modulation can be described by a single wave vector  $q_+$  or  $q_-$  in the temperature domain 49-38 K. However, a transverse commensurability ( $\times 4$ ) arises abruptly at 38 K. The ordering of the charge density modulations both along **a** and **b** directions at 36.5 K is presented in figs.3c,d. Below 38K (low temperature commensurate phase) a double- $q$  CDW modulation  $q_+$  and  $q_-$  is identified.

The images presented above are the first to report a study of the 2D superlattice structure of TTF-TCNQ in real space below the Peierls transition down to the temperature of 33 K. The value and temperature dependence of the modulation wave vector are in very good agreement with the detailed X-ray [6, 15, 16] and neutron scattering [17, 18] reports (see fig.4a).

We can provide a real space signature of the intermediate temperature regime in which the transverse period is evolving with temperature (the sliding regime) before a lock-in takes place at 38 K. Although the signal coming from the CDW modulation is always dominant in all our scans (with a corrugation of 0.21 nm at 36.5 K along the TCNQ stacks) it does

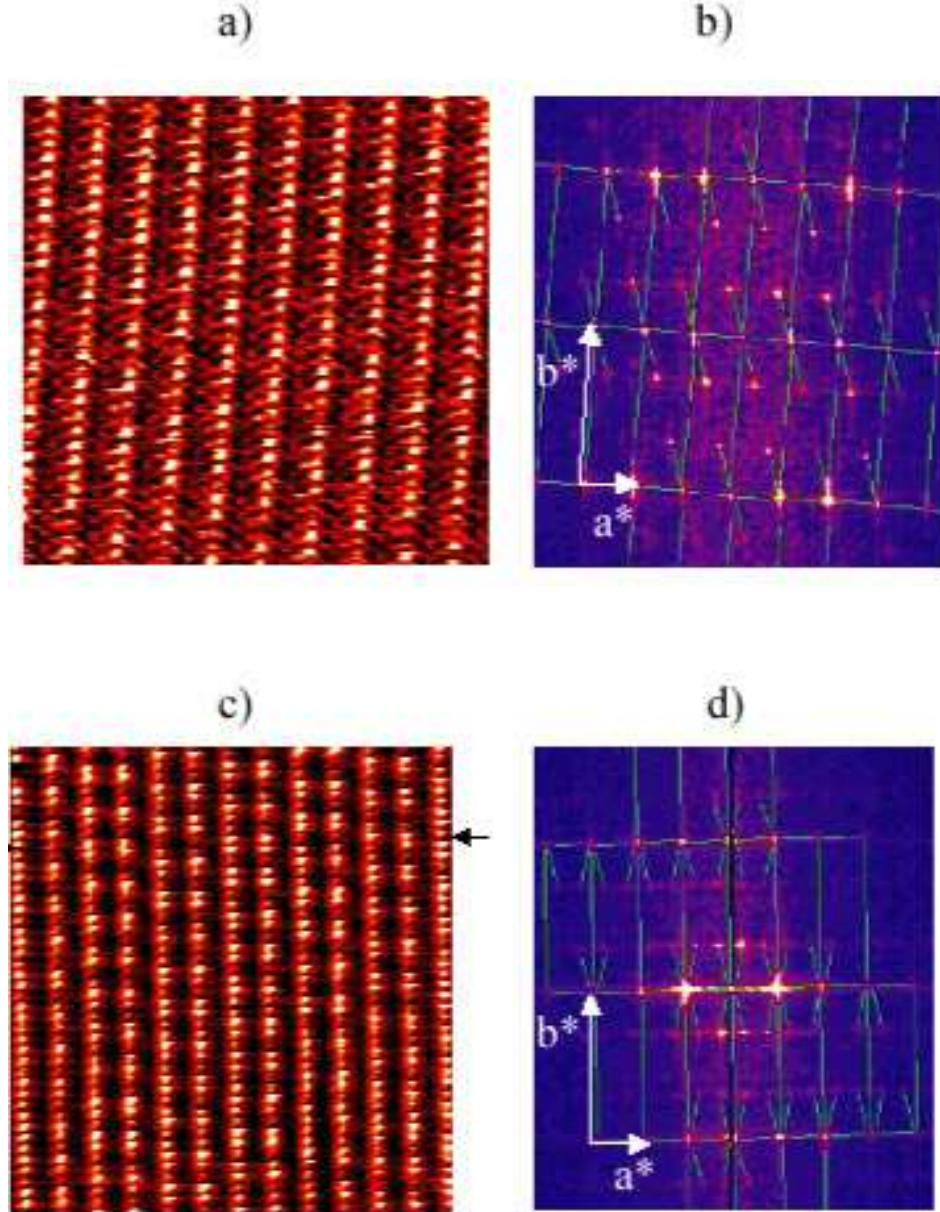


FIG. 3: a) STM image of the  $\mathbf{a}$ - $\mathbf{b}$  plane of TTF-TCNQ taken at 39K, the image area is 9.3 nm x 6.9 nm, b) Fourier transformed pattern showing the single-q CDW in the sliding temperature domain, c) STM image of the  $\mathbf{a}$ - $\mathbf{b}$  plane of TTF-TCNQ taken at 36.5K, the image area is 14.8×14.7 nm, d) Fourier transformed pattern showing the double-q ( $4\mathbf{a}\times 3.3\mathbf{b}$ ) CDW in the commensurate phase.

not overcome the corrugation coming from the underlying TCNQ lattice, namely 0.12 nm. Thanks to the coexistence between CDW and original lattices on the images, molecular resolution can be obtained in the CDW condensed state at low temperature.

This is *at variance* with layered compounds such as 1T-TaSe<sub>2</sub> where the image is domi-

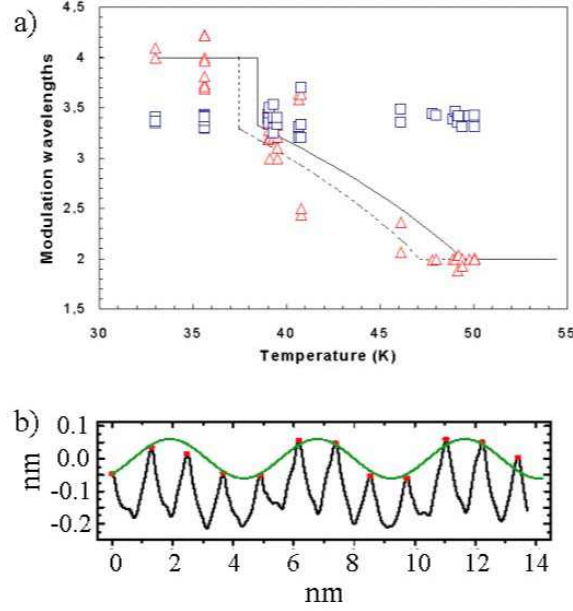


FIG. 4: a) Temperature dependence of the CDW wavelengths along **a** (triangles) and **b** (open squares) directions in unit cell dimensions. The large scattering of the data at  $T=40.6\text{K}$  were taken from small images of  $5\text{ nm}\times 5\text{ nm}$  while other temperatures were taken from images larger than  $10\text{ nm}\times 10\text{ nm}$ . The solid (dotted) lines are obtained from X-rays diffraction measurements in warming (cooling) respectively. b) Cosine fit of the CDW profile at  $36.5\text{K}$  along the **a** direction indicated by black arrows in fig. 3c revealing the CDW phasing.

nated by the CDW superlattice but somewhat similar to the situation in  $2\text{H-NbSe}_2$  [19].

The very good agreement between the real space CDW features and the results from the neutron scattering experiments shows that cleaved surfaces are highly ordered and retain the electronic properties of the bulk material. A similar conclusion was reached in ARPES experiments performed on cleaved (001) surfaces of TTF-TCNQ [20, 21]. The salient result of this work is given in fig.3 which makes it clear that warming through the transverse lock-in transition the modulation evolves from an amplitude modulation along **a** (double- $q$  superlattice) in the commensurate phase to a phase modulation in the incommensurate wave vector regime with only a single- $q$  vector activated over the investigated sample area.

Thus, we have shown that TTF-TCNQ adopts a domain structure in the temperature regime where the transverse ordering of the CDW's is incommensurate. This is probably the clue to understand the hysteresis displayed by  $q_a(T)$  between  $49\text{K}$  and  $38\text{K}$  [17, 18] as suggested by [22, 23].

The fact that the CDW is observable by a STM probe shows that it is static in spite of its incommensurate nature (along the  $\mathbf{b}$  direction), and is therefore pinned by impurities or defects .

The low temperature CDW in TTF-TCNQ is thus an ideal candidate to study the local phase shift for the following reasons: the unit cell in the  $\mathbf{a-b}$  plane has a quadratic symmetry, the CDW phase is commensurate in the  $\mathbf{a}$  direction but incommensurate in the  $\mathbf{b}$  direction, the CDW modulation is double- $q$  modulated below 38K so the phase shifts along  $\mathbf{a}$  and  $\mathbf{b}$  can be studied separately and in addition a modulation of the amplitude along  $\mathbf{a}$  is expected.

Furthermore, we notice on figs.4a,b that the phase of the CDW is such as to present an alternation of the amplitude on the TCNQ stacks like  $++--++$ , etc... along the  $\mathbf{a}$  direction.

The phasing of the CDW with respect to the underlying lattice below 38 K agrees with the diffraction experiments data [15]. The results of our work show that STM techniques are very well adapted to the local study of CDW's in TTF-TCNQ and resolve the question of phase against amplitude modulation. In addition, this work opens new ways towards a local investigation of the pinning of the CDW's around impurities to derive information about the nature of the pinning mechanism (strong or weak).

We thank J.P.Pouget, K.Maki and E.Canadell for very fruitful discussions.Z.Z.Wang acknowledges the financial support of the SESAME contract 1377.

- 
- [1] L.B.Coleman et al. *Solid State.Comm*, 12:1125, 1973.
  - [2] J.P.Ferraris et al. *J.Am.Chem.Soc*, 95:948, 1973.
  - [3] D.J erome and H.J.Schulz. *Advances in Physics*, 31:299, 1982.
  - [4] A.Bjeli  and S.Bari i  . *Phys.Rev.Lett*, 37:1517, 1976.
  - [5] E.Abrahams, J.Solyom, and F.Woynarovich. *Phys.Rev.B*, 16:5238, 1977.
  - [6] S.Kagoshima, T.Ishiguro, and H.Anzai. *J.Phys.Soc.Japan*, 41:2061, 1976.
  - [7] Y.Bouveret and S.Megtert. *J.Physique.France*, 50:1649, 1989.
  - [8] T.Nishiguchi et al. *Phys.Rev.Lett*, 81:3187, 1998.
  - [9] P.Bak and V.J.Emery. *Phys.Rev.Lett*, 36:978, 1976.
  - [10] T.J.Kistenmacher, T.E.Phillip, and D.O.Cowan. *Acta Cryst B*, 30:763, 1974.



- [11] T.Sleator and R.Tycko. *Phys.Rev.Lett*, 60:1418, 1988.
- [12] N.Kato et al. *Nanotechnology*, 7:122, 1996.
- [13] P.Ordejon, E.Canadell, Y.J.Lee, and R.Nieminen. *to be published*.
- [14] W.Sacks, D.Roditchev, and J.Klein. *Phys.Rev.B*, 57:13118, 1998.
- [15] J.P.Pouget. *in: Semiconductors and Semimetals*, page 87. Academic Press, 1988.
- [16] S.K.Khanna et al. *Phys.Rev.B*, 16:1468, 1977.
- [17] W.D.Ellenson et al. *Solid.State.Comm*, 20:53, 1976.
- [18] W.D.Ellenson et al. *Phys.Rev.B*, 16:3244, 1977.
- [19] B.Giambattista et al. *Phys.Rev.B*, 37:2741, 1988.
- [20] F.Zwick et al. *Phys.Rev.Lett*, 81:2974, 1998.
- [21] R.Claessen et al. *Phys.Rev.Lett*, 88:096402, 2002.
- [22] J.P.Pouget and R.Comes. *in: Charge Density Waves in Solids*, page 85. eds. L.P.Gork'ov and G.Grüner, Elsevier, 1989.
- [23] S.Barišić and A.Bjeliš. *in: Theoretical Aspects of Band Structure and Electronic Properties of Pseudo-One-Dimensional Solids*, page 49. D.Reidel PublishingCompany, 1985.